UNIVERSITYOF
BIRMINGHAM

Design, modelling and validation of a linear Joule Engine generator designed for renewable energy sources

Jia, B.; Wu, Dawei; Smallbone, A.; Lawrence, Chris; Roskilly, A.P.

Link to publication on Research at Birmingham portal

Design, modelling and validation of a linear Joule Engine generator designed for renewable energy sources

Jia, Boru; Wu, Dawei; Smallbone, Andrew; Lawrence, Chris; Roskilly, Anthony Paul

Link to publication on Research at Birmingham portal

1 **Design, Modelling and Validation of a Linear Joule Engine Generator designed**

2 **for Renewable Energy Sources**

3 Boru Jia[a*]; Dawei Wu[b]; Andrew Smallbone[a]; Chris Lawrence[a]; Anthony Paul Roskilly[a]

4 [a] Sir Joseph Swan Centre for Energy Research, School of Engineering, Newcastle University, Newcastle upon Tyne, NE1 7RU, UK

5 [b] Marine, Offshore and Subsea Technology, School of Engineering, Newcastle University, Newcastle upon Tyne, NE1 7RU, UK

6 **Abstract**

7 The Linear Joule Engine Generator (LJEG) incorporates the Joule Engine technology and the

8 permanent magnet linear alternator design, which is a promising power generation device for the

9 applications of range extenders for electric vehicles, Combined Heat and Power (CHP) systems, or as

10 a stand-alone power unit. It combines the advantages from both a Joule Engine and a linear alternator,

11 *i.e.* high efficiency, compact in size, and flexible to renewable energy integration, etc. In this paper,

12 the background and recent developments of the LJEGs are summarised. A detailed 0-dimentional

13 numerical model is described for the evaluation of the system dynamics and thermodynamic

14 characteristics. Model validation is conducted using the test data obtained from both a reciprocating

15 Joule Engine and a LJEG prototype, which proved to be in good agreement with the simulation results.

16 The fundamental operational characteristics of the system were then explained using the validated

17 numerical model. It was found that the piston displacement profile has certain similarity with a

18 sinusoidal wave function with an amplitude of 51.0 mm and a frequency of 13 Hz. The electric power

19 output from the linear alternator can reach 4.4kW$_e$. The engine thermal efficiency can reach above

20 34%, with an electric generating efficiency of 30%.

21 **Keywords:** Linear Joule-cycle Engine; linear expander; linear alternator; numerical model; model

22 validation.

23 * Corresponding author: Boru Jia

24 Email: boru.jia@newcastle.ac.uk; jiaboru@sina.com; Tel: +44 07547839154

25

26 **1. Introduction**

27 The Linear Joule Engine Generator (LJEG) is derived from the Joule Engine technology and

28 incorporates a permanent magnet in a linear alternator design. The Joule Engine technology uses a free

29 piston configuration with a potential high efficiency due to its mechanical simplicity and minimal

frictional loss, in addition it employs an external (out-of-cylinder) heat addition method to adapt to various renewable energy sources [1-3]. The permanent magnet linear alternator is reported to be compact in size, and efficient in electricity generation [4-7]. The LJEG takes advantages of both a Joule Engine and the Linear Engine Generator, and it provides an alternative high-efficiency, renewable energy adaptive, prime mover for transportation and power generation applications. At the same time, it offers flexibility at a time when it is expected to see a major increase in the low-carbon/carbon-free fuel variety, e.g. biogas, biofuels, hydrogen and ammonia, in these sectors towards 2050.

1.1 Joule Engine technology

The Joule cycle (or Brayton Cycle) is widely employed in gas turbines, where air intake is compressed, before fuel is burnt under constant pressure, and then, the exhaust gas expands out to ambient pressure. Typically the compression and expansion processes are performed by turbomachinery [8]. In theory it has isobaric heat addition and heat rejection processes, and isentropic compression and expansion. The reciprocating Joule Engine technology applies split a reciprocating compressor and expander to improve its efficiency, which was proposed as an engine for application in the micro CHP systems [1, 3, 9].

Moss *et al.* estimated the performance of a Joule Engine in small size (1-10 kW) with a simple simulation model in Matlab [1]. M. Alaphilippe, *et al*. provided a theoretical investigation on the coupling of a two-stage parabolic trough solar concentrator with a hot air Joule Engine [10]. The preliminary results were reported to be promising of coupling a simple parabolic though and a Joule Engine. Wojewoda and Kazimierski provided investigation on operation of an externally heated valve Joule Engine [11]. A numerical model was presented, and the heat exchanger operation was further investigated. M. Creyx, *et al.* developed a numerical model of an open cycle Joule Engine, which was focused on the thermodynamic aspects [12]. The reported system thermodynamic efficiency was 37%

54 after some optimisation work. Bell and Partridge presented a first-order model of a Joule Engine, and

55 the model included combustion, clearance volume, gas leakage, pressure drop, and friction [2].

56 Another system was reported by the researchers at Plymouth University, the system power output and

57 efficiency were simulated, indicating an engine thermal efficiency of up to 33% [2]. The model

58 validation was performed using the testing results of both a demonstration engine and a prototype

59 engine [13].

60 **1.2 Linear Engine Generator technology**

61 The Linear Engine Generator is linear 'crank-less' power device that couples a linear internal

62 combustion engine with a linear electric generator, it uses conventional diesel or Otto cycles [4, 14,

63 15]. The piston of the engine is connected with the translator of the generator. Combustion takes place

64 in the engine cylinder, and the high pressure gas during the expansion process is used to drive the

65 piston and the translator, and the linear generator produces electricity [16]. There have been different

66 prototypes reported by different research groups [17-23]. Sucessful implementations of single cylinder

67 Linear Engine Generators have been reported by Toyota Central R&D Labs Inc. and the German

68 Aerospace Centre (DLR), which were both composed of a single cylinder engine, a linear electric

69 generator, and a gas spring rebound chamber [23-26]. For the prototype developed at DLR, it was

70 operated at 21 Hz, with an electric power output of approximately 10 kW [27]. The TDC achieve was

71 found to be at 57.5% of the periodic time [28]. For the dual-piston dual-cylinder Linear Engine

72 Generator, several prototypes have been designed in Beijing Institute of Technology [6, 7]. Both 0/1

73 dimensional and multi-dimensional simulation were undertaken to predict the dynamic and

74 thermodynamic performance of the system [29-31]. Successful engine cold start-up has been reported,

75 and the combustion took place when the cylinder pressure reached the required level for ignition [7,

76 32, 33]. The piston was controlled to oscillate between two set positions with constant speed [34, 35].

77 The predicted system efficiency was around 35%. The potential disturbances to the system were

78 analysed, and a cascade control strategy was proposed for the piston stable control [36, 37].

1.3 Linear Joule Engine Generator development

The Linear Joule Engine Generator concept was first proposed by the authors' group, initially aiming for application for micro-scale CHP generation [3]. Simple calculations were undertaken, and the simulation results suggested that a domestic CHP plant based on the proposed technology could reach an electric generating efficiency of above 30%. With a heating temperature of around 1100 K and a compressor outlet pressure of 6 bar, the engine could produce 4.5 kW of mechanical power. Whilst, through waste heat recovery technology, the total system could reach a promising efficiency of over 90%. Later on, a 3-dimentional diagram of the proposed LJEG system was presented by the authors [9]. The geometry parameters of the system were optimised in LMS AMESim software, which provided a solid basis for the manufacturing of the prototype. Meanwhile, Wu et al. presented a coupled dynamic model of the Linear Joule Engine and the connected permanent magnet linear electric generator, aiming to provide a better prediction of the system performance. It was estimated that the LJEG system could generate 1.8 kW electricity, with an engine thermal efficiency of 34% and electric generating efficiency of 30% [38].

1.4 Aims and methodology

In this research, the background and recent developments of the LJEG are summarised. A more detailed numerical model of the system will be described, which includes the sub-models for the piston dynamics, the reactor, the linear expander, the linear compressor, and the linear generator, etc. The model validation will be performed with the testing data from both a reciprocating Joule Engine, and a LJEG prototype developed by the authors' group. The system dynamics and thermodynamics characters will be identified with the validated model.

2. System configuration

For an ideal Joule Engine Cycle (as illustrated in Figure 1), it usually consists of four processes, *i.e.* adiabatic compression process in the compressor, constant pressure fuel combustion process, adiabatic expansion process in the expander [39]. It should be noted that the "Combustor" shown in Figure 1 can be replaced with any fuel combustion, waste heat, or renewable energy reaching certain temperature, and the gas will drive the expander.
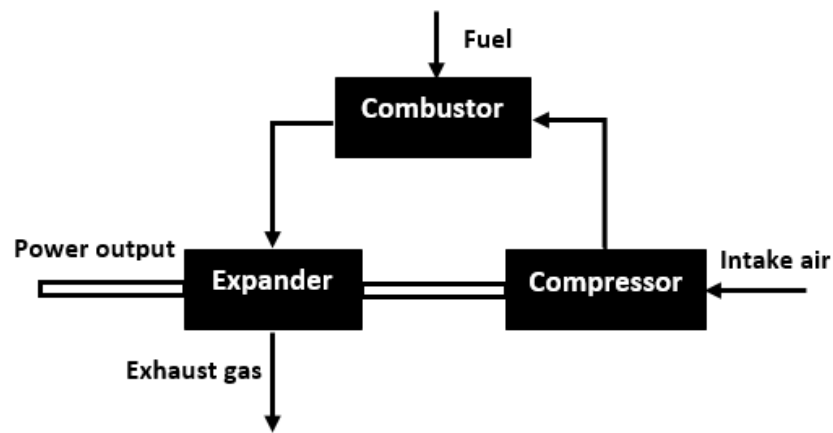
Figure 1. System schematic figure of a Joule Engine Cycle

The configuration of the LJEG prototype developed by the authors is illustrated in Figure 2, using an external reactor to burn fuel as heat input. It is an open system, and the exhaust gas after the expander would be high-pressure, high temperature gas. The air is compressed in a positive displacement compressor featured with a double-acting free piston and several poppet valves for intake and discharge; the compression of the air results in a high pressure, high temperature air, which is fed into an external reactor. The fuel is fed into the reactor and reacts with the air to produce heat and high pressure gas. The expander reduces the pressure and temperature by expanding the working fluid and this expansion is used to drive the linear generator and the compressor.

6

116
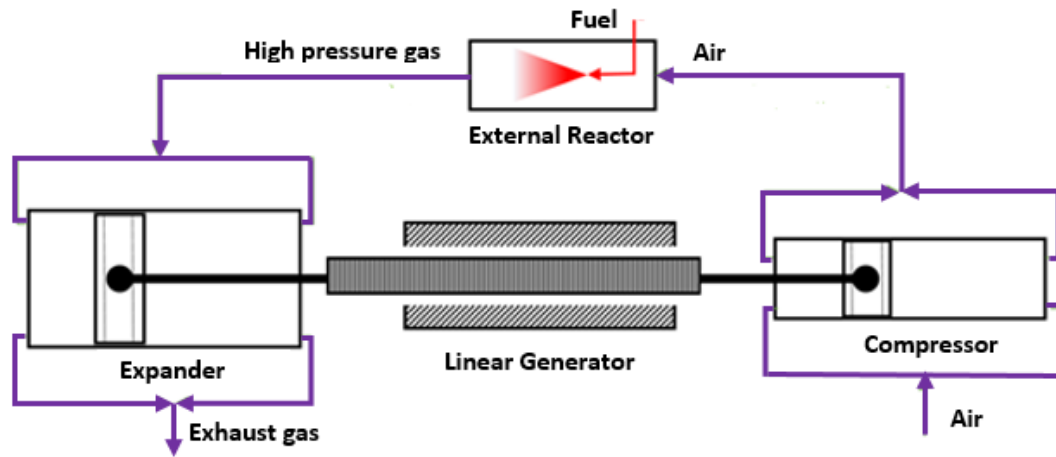
Figure 2. The LJEG prototype configuration with a reactor as an example heat input

3. Numerical modelling

3.1 Model structure

The numerical model aims to describe the dynamic and thermodynamic characteristics of the LJEG system, e.g. the piston motion, the pressure variation in the expander and the compressor, the system power output, the system efficiency, etc. As the piston in the proposed system is not restricted by a mechanical linkage, the piston motion is determined by the forces acting on it, which are the gas pressure forces from the linear expander and the compressor, the resistance force from the linear generator, the frictional force, and the inertia of the moving mass. Therefore a piston dynamic model is developed on the top level. The structure of the numerical model is demonstrated in Figure 3.

Three sub-model that describe the specific forces that acting on the pistons are developed on a lower level, and the calculated forces are used as feedback signals to the top-level piston dynamic model to determine the piston acceleration. The pressure forces are determined by the gas thermodynamic processes from both chambers of the linear expander and the linear compressor, which consider the compression/expansion of the piston, gas intake/exhaust through the valves, the heat transfer from the

132 gas of the chamber to the wall, etc. During the operation of the system, the linear generator will

133 generate electricity, and outputs an electric resistance force acting on the piston.

134 The performance of the linear expander is affected by the high-pressure, high-temperature gas from

135 the external reactor, which is the intake gas to the chambers of the expander through the intake valves.

136 The outputs of the reactor, *i.e.* the gas pressure, temperature, and mass flow rate, will be used as input

137 parameters to the linear expander during the gas intake process. The external reactor can be replaced

138 with any fuel combustor, solar energy, waste heat, or renewable energy that can drive the expander.

139 The external reactor would largely follow the isobaric heat addition process with a confined pressure

140 fluctuation regardless fuel species, thus the inlet pressure and temperature of the linear expander are

141 assumed to be constant.
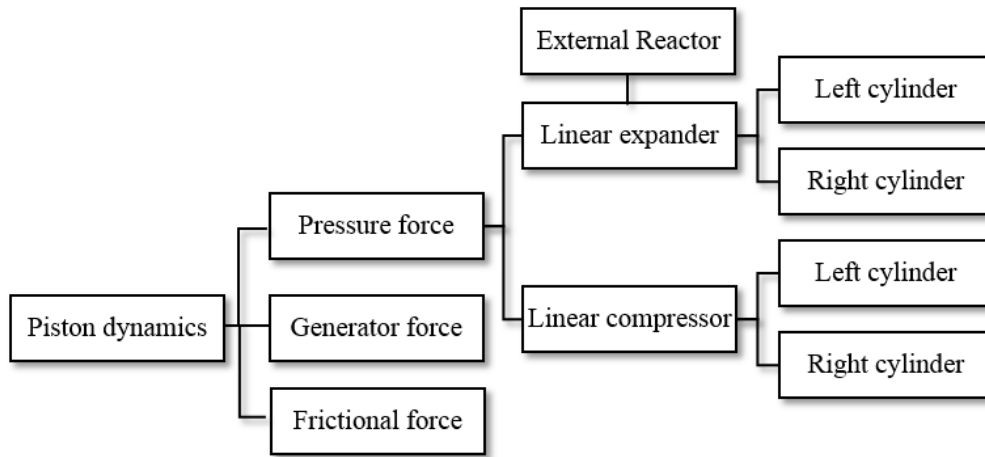
142

143 <p align="center">Figure 3. The structure of the numerical model</p>

144 **3.2 Piston dynamics model**

145 The forces acting on the pistons are the gas pressure forces from the linear expander and the

146 compressor, the resistance force from the linear generator, the frictional force, and the inertia of the

147 moving mass, which can be expressed as blow according to the Newton's Second Law:

148
$$\overrightarrow{F_{exp}} + \overrightarrow{F_{com}} + \overrightarrow{F_e} + \overrightarrow{F_f} = m\ddot{x} \tag{1}$$

$$\overrightarrow{F_{exp}} = \overrightarrow{F_{exp\_l}} + \overrightarrow{F_{exp\_r}} \qquad (2)$$

149

$$\overrightarrow{F_{com}} = \overrightarrow{F_{com\_l}} + \overrightarrow{F_{com\_r}} \qquad (3)$$

150

151 Where $\overrightarrow{F_{exp}}$ (N) is the pressure force from the linear expander; $\overrightarrow{F_{exp\_l}}$ (N) is the pressure force from the

152 left chamber of the linear expander; $\overrightarrow{F_{exp\_r}}$ (N) is the pressure force from the right chamber of the linear

153 expander; $\overrightarrow{F_{com}}$ (N) is the pressure force from the linear compressor; $\overrightarrow{F_{com\_l}}$ (N) is the pressure force

154 from the left chamber of the linear compressor; $\overrightarrow{F_{com\_r}}$ (N) is the pressure force from the right chamber

155 of the compressor; $\overrightarrow{F_e}$ (N) is the resistance force from the linear electric alternator; $\overrightarrow{F_f}$ (N) is the

156 frictional force.

157 The gas forces from both chambers of the linear expander and compressor can be calculated by the gas

158 pressure and piston effective area, where can be represented as following:

$$\overrightarrow{F_{exp\_l}} = p_{\exp\_l} \cdot A_{exp} \qquad (4)$$

159

$$\overrightarrow{F_{exp\_r}} = p_{\exp\_r} \cdot A_{exp} \qquad (5)$$

160

$$\overrightarrow{F_{com\_l}} = p_{\mathrm{com}\_l} \cdot A_{com} \qquad (6)$$

161

$$\overrightarrow{F_{com\_r}} = p_{\mathrm{com}\_r} \cdot A_{com} \qquad (7)$$

162

163 Where $p_{\exp\_l}$ (Pa) is the cylinder pressure from the left chamber of the linear expander; $p_{\exp\_r}$ (Pa) is

164 the cylinder pressure from the right chamber of the linear expander; p_{com_l} (Pa) is the cylinder pressure

165 from the left chamber of the linear compressor; p_{com_r} (Pa) is the cylinder pressure from the right

166 chamber of the linear compressor; A_{exp} (m^3) is the piston area of the expander; A_{com} (m^3) is the piston

167 area of the compressor.

168 **3.3 Linear expander**

169 The thermodynamic processes in a chamber of the linear expander mainly include the

170 compression/expansion process due to the piston movement, heat transfer from gas in the chamber to

171 the wall, as well as the inlet and exhaust gas exchange processes. By applying the first law of

172 thermodynamics on the charge in the chamber and ideal gas equation, yields the pressure calculation

173 equation for one of the two chambers (detailed derivation process can be found in the previous

174 publications of the authors [25]):

$$\frac{dp_{exp}}{dt} = \frac{\gamma-1}{V_{exp}}\left(-\frac{dQ_{ht}}{dt}\right) - \frac{p_{exp}\gamma}{V_{exp}}\frac{dV_{exp}}{dt} + \frac{\gamma-1}{V_{exp}}\sum_i \dot{m}_{expi}\, h_{expi} \qquad (8)$$

176 Where p_{exp} is the pressure in the chamber of the linear expander (pa); γ is the heat capacity ratio; V_{exp}

177 is the working volume of the linear expander for one cylinder (m^3); $\dot{m}_{expi}$ is the mass flow rate in or

178 out of the valve (m/s); h_{expi} is the specific enthalpy of the mass flow (J·kg^{-1}).

179 The heat transfer between the walls and the gas of one chamber of the expander is modelled according

180 to Hohenber [40]:

$$\dot{Q}_{ht} = 130V^{-0.06}\left(\frac{p(t)}{10^5}\right)^{0.8} T^{-0.4}\left(v_p + 1.4\right)^{0.8} \cdot A_{exp\_surf}(T - T_w) \qquad (9)$$

182 Where $\dot{Q}_{ht}$ is heat flow rate (J/s); V is the instantaneous cylinder volume (m^3); v_p is the average piston

183 speed (m/s), A_{exp_surf} (m^2) is area of the surface in contact with the gas in the chamber of the expander;

184 T_w (K) is the average surface temperature of the cylinder wall.

185 The mass flow rate through the valves, $\dot{m}_{flow}$ is assumed to be represented by a compressible flow

186 through a flow restriction. It is determined by temperature, composition, the gas pressure, and a

187 reference area of the valve [24], which is given by:

$$\dot{m}_{flow} = \begin{cases} \frac{C_d A_d p_u}{(RT_u)^{\frac{1}{2}}} \left(\frac{p_d}{p_u}\right)^{\frac{1}{\gamma}} \sqrt{\frac{2\gamma}{\gamma-1}\left[1 - \left(\frac{p_d}{p_u}\right)^{\frac{(\gamma-1)}{\gamma}}\right]}, & p_d/p_u > [2/(\gamma+1)]^{\gamma/(\gamma-1)} \\ \frac{C_d A_d p_u}{(RT_u)^{1/2}} \gamma^{1/2} \left(\frac{2}{\gamma+1}\right)^{(\gamma+1)/2(\gamma-1)}, & p_d/p_u \le [2/(\gamma+1)]^{\gamma/(\gamma-1)} \end{cases} \tag{10}$$

188

Where $\dot{m}_{flow}$ is the mass flow rate through a poppet valve (kg/s); C_d is the discharge coefficient; A_d is

the reference area of the flow (m²); T_u is the temperature of the upstream of the flow restriction (K);

p_u is the pressure of the upstream of the flow restriction (Pa); p_d represents the downstream air

pressure of the flow restriction (Pa).

3.4 Linear compressor

For ideal gas, both compression and expansion process are governed by the gas pressure and its volume

after the intake valve and exhaust valve closed. The air leakage across the piston rings was considered

negligible, hence it is assumed that the gas is completely isolated by the piston rings and there is no

air mass transfer. The relationship between gas pressure p_{com} and volume of the chamber V_{com} during

the compression/expansion process is listed below:

$$\frac{dp_{com}}{dt} = \frac{\gamma-1}{V_{com}}\left(-\frac{dQ_{ht}}{dt}\right) - \frac{p_{com}\gamma}{V_{com}}\frac{dV_{com}}{dt} \tag{11}$$

Where p_{com} is the pressure in the chamber of the linear compressor (pa); γ is the heat capacity ratio;

V_{com} is the working volume of the linear compressor for one cylinder (m³).

The intake and exhaust valves here adopted are reed valves, which open when the pressure of the

upstream is higher than that of the downstream. When the intake valve is opened, the gas pressure in

the chamber of the linear compressor is assumed to be equal with the intake pressure immediately; and

the gas pressure is assumed to be same with the exhaust pressure (or the intake pressure to the linear

expander) once after the exhaust valve is open. In summary, the gas pressure in one chamber of the

linear compressor is described by:

11

208
$$p_{com\_2} = \begin{cases} p_{exp\_in}; & p_{com\_2} > p_{exp\_in} \\ p_{com\_1}(V_{com\_1}^\gamma/V_{com\_2}^\gamma); & p_{com\_in} < p_{com\_2} < p_{exp\_in} \\ p_{com\_in}; & p_{com\_2} < p_{com\_in} \end{cases} \qquad (12)$$

209   Where p_{com_in} (Pa) is the intake gas pressure of the linear compressor; p_{exp_in} (Pa) is the intake gas

210   pressure of the linear expander, which is the same with the exhaust gas pressure of the linear

211   compressor.

212   **3.5 Linear electric generator**

213   The linear electric machine is operated as a generator, electrical current is drawn from the alternator

214   coils through the continuous back and forth movement of the mover. The linear generator is modelled

215   using a simplified numerical model to make it feasible with limited amount of design parameters

216   known to the users. Figure 4 illustrates an equivalent circuit of the linear electric machine.

217
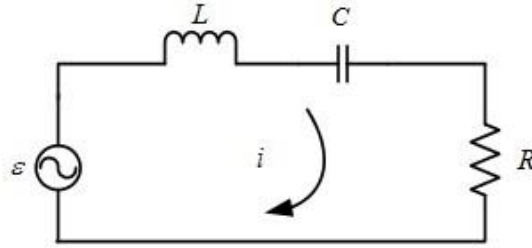
218   Figure 4 Equivalent circuit of the linear electric machine [31]

219   Then the Faraday's electromagnetic induction laws give the electromotive voltage ε (V) as

220
$$\varepsilon(t) = -N\frac{d\emptyset}{dt} = -K_v\frac{dx}{dt} = -K_v \cdot v \qquad (13)$$

221   Where $\emptyset$ is the magnetic flux; K_v is a motor property and determined by the design parameters of the

222   motor and can be found in the manual; x is the piston displacement (m); v is the piston velocity (m/s).

223   The induced current is determined by the voltage and the load circuit, assuming the load circuit is

224   purely resistive ($C = 0, L = 0$), it can be derived by:

225
$$\varepsilon(t) = (R_S + R_L)i(t) \qquad (14)$$

226   Where R is the resistance of the circuit (Ω), R_S is the internal resistance (Ω), and R_L is the resistance of

227   the external load (Ω); i is the current (A).

228   Then the current in the coil is then expressed by:

$$i(t) = -\frac{K_v}{R_S + R_L} \cdot v \tag{15}$$

230   As the load force of the electric machine is assumed to be proportional to the current of the circuit

231   according to electromagnetic theory, the resistance force from the alternator is then written as:

$$F_e = -C_e v \tag{16}$$

233   Where C_e is the load constant of the alternator (N/(m·s^{-1})), which can be calculated from the physical

234   parameters of the alternator design specifications.

3.6 Frictional force

236   An analysis of engine friction mechanisms in four stroke spark ignition and diesel engines is presented

237   by Heywood [41]. Friction work is expected to be lower than conventional internal combustion engines

238   due to the elimination of the crank mechanism. Thus the friction in the wrist pin, big end, crankshaft,

239   camshaft bearings, the valve mechanism, gears, or pulleys and belts which drive the camshaft and

240   engine accessories have been removed. The total friction force F_f of each piston is estimated as a linear

241   combination of piston velocity plus a constant C_s, as shown in the equation below [42]:

$$F_f = -(C_k \cdot |v| + C_s) \cdot sign(v) \tag{17}$$

243   C_k is the kinetic friction coefficient related to the instantaneous velocity, and the C_s is the static

244   friction coefficient as a constant part of the frictional force.

4. Model implementation and validation

4.1 Simulation model implementation

The simulation model is developed in Matlab/Simulink. The design parameters of the model are derived from the preliminary design of the prototype in built/testing and the initial boundary conditions are defined based on the practical starting conditions and the assumptions made in the model mentioned above. Both the piston displacement and velocity generated in the simulation are monitored and fed back to a controller which imposes the valve timings. The initial piston position is assumed to be at its TDC (approximately 8 mm from the cylinder head) in the left chamber of the linear expander.

The prototype specifications and the values of the input parameters for the system operation cycles are listed in Table 1. The system design parameters and the input boundary parameters will be further optimised at the next stage. The inlet pressure of the reactor is set to be the same with the outlet pressure of the linear compressor, and the inlet pressure of the linear expander, which can be adjusted during the simulation. The outlet pressure of the linear compressor, and the mass flow rate to the reactor are all variables, which will affect the inlet pressure to the reactor and the linear expander, and the intake temperature of the linear expander correspondingly.

Components	Parameters [Unit]	Value
Expander	Moving mass [kg]	8.5
	Maximum stroke [mm]	120.0
	Effective bore [mm]	80.0
	Inlet pressure [bar]	7.0
	Inlet temperature [K]	1100.0
	Valve number	4
	Valve diameter [mm]	32.5
	Valve lift [mm]	8.13
Linear compressor	Maximum stroke [mm]	120.0

14

	Effective bore [mm]	66.0
	Inlet pressure [bar]	1.0
	Outlet pressure [bar]	7.0
Linear generator	load constant [N/m·s^{-1}]	367.6

260   Table 1. Prototype specifications and input parameters

261   As the valves are actuated based on the piston position, the scavenging durations will be significantly

262   affected by the piston speed and profile. The step functions are used to impose the valve-lift profiles,

263   as which proved to be aligned with the response of the installed valve system. The opening and closing

264   valve timings can be adjusted via the controller to optimise the scavenging process. The expansion

265   process of the expander is initialised after the intake valve open (IVO), which is actuated when the

266   piston reaches its TDC. The exhaust valve open (EVO) is triggered when the piston reaches its BDC.

267   The valve timings versus the piston displacement for both chambers of the expander are illustrated in

268   Figure 5, and example piston dead centres are set to -50 mm and 50 mm.

269
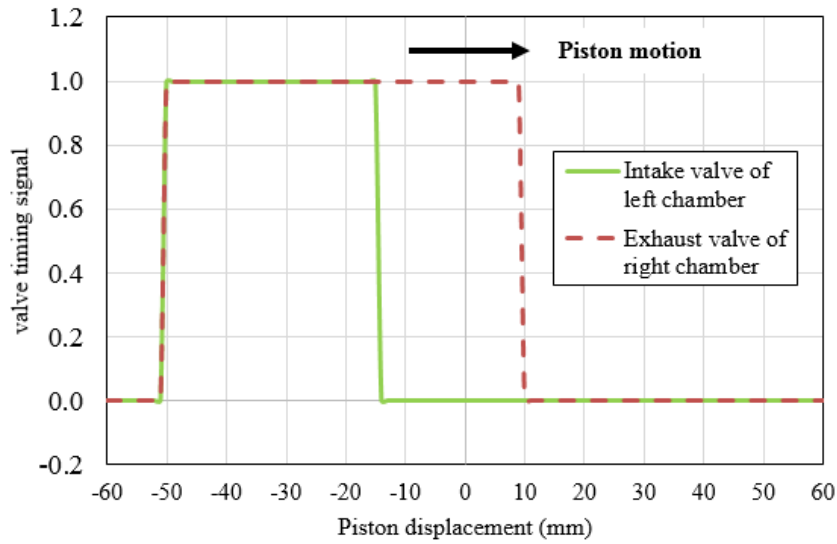
270   (a) Rightward stroke

15
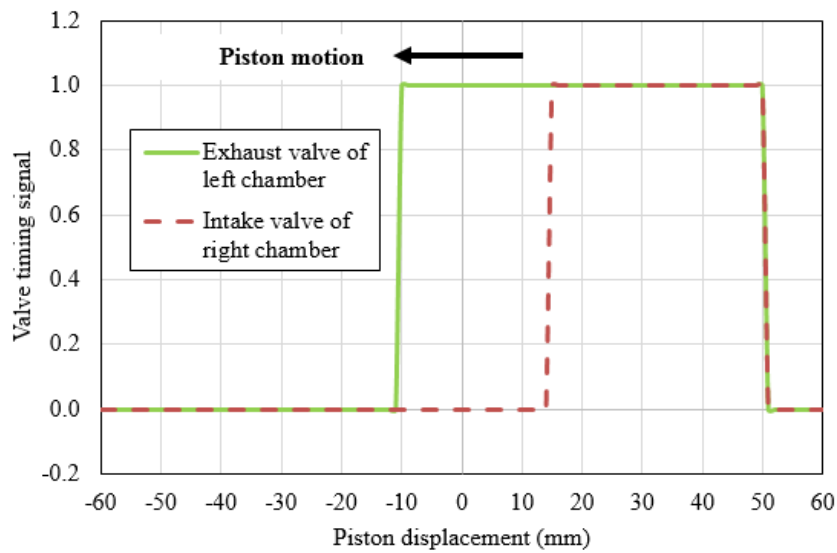
(b) Leftward stroke

Figure 5. The example valve timings for both chambers of the linear expander

4.2 Validation with a Reciprocating Joule Engine

The simulation results from the model were first compared to data from a Reciprocating Joule Engine

developed at University of Plymouth [8]. The configuration of a Reciprocating Joule Engine is

different from the LJEG system, which is illustrated in Figure 6. The comparison was undertaken to

verify that the simulation developed in this research produces the realistic results and is valid for

predicting the prototype performance in different system operation conditions. The system

specifications were set to be identical with the Reciprocating Joule Engine introduced in [8]. The

Reciprocating Joule Engine input parameters are listed in Table 2, the bores of the expander and

compressor are the same.
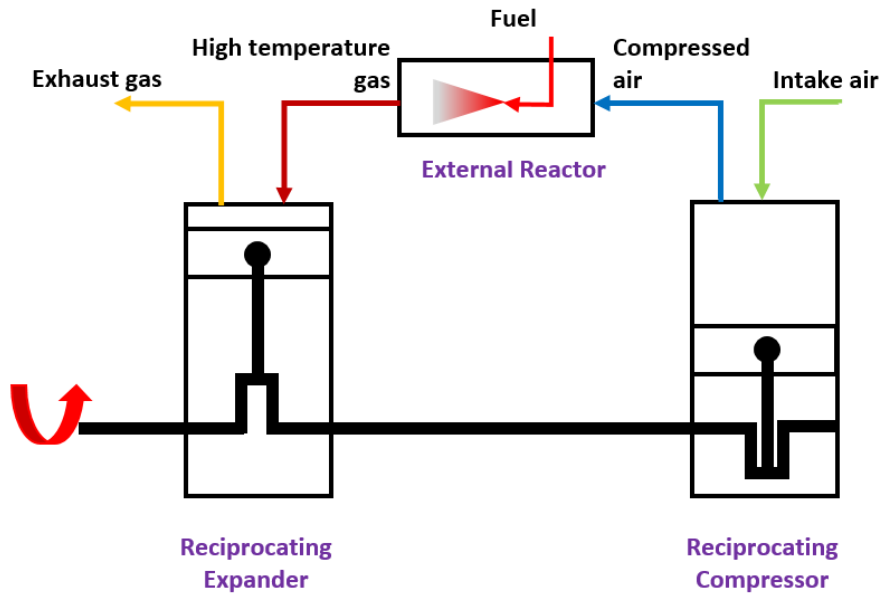
284   Figure 6. Schematic configuration of a Reciprocating Joule Engine

Parameter [Unit]	Value
Stroke [mm]	61.5
Bore [mm]	82.0
Clearance volume [cc]	30
Supply pressure [bar]	7.5
Supply temperature [K]	850

285   Table 2. The Reciprocating Joule Engine specification for model validation [8]

286 During the testing, the engine was operated on external compressed air (with no compressor connected).

287 The test data and simulation results of the expander pressure are compared in Figure 7. For the

288 Reciprocating Joule Engine, the expander was operated on external compressed air, and the

289 compressor was not connected, which would contribute to the difference with the simulation results.

290 The valve timing was set based on the crank angle, and the inlet valve was set to open at 10º before

291 TDC, and close at 80º after TDC. The exhaust valve was set to open at 10º before BDC, and close at

292 70º before TDC [8]. As for the LJEG concept used in this research, the piston is not restricted with

293 mechanical crankshaft linkage, and the piston movement cannot be represented with crank angle as

294   the Reciprocating Joule Engine does. As a result, the setting of the valve timing in the simulation

295   would not be exactly the same with the test engine, which introduces the error to a great extent. Despite

296   of the errors, the numerical model can simulate the performance of the expander, and predict the

297   variation of the cylinder pressure.

298
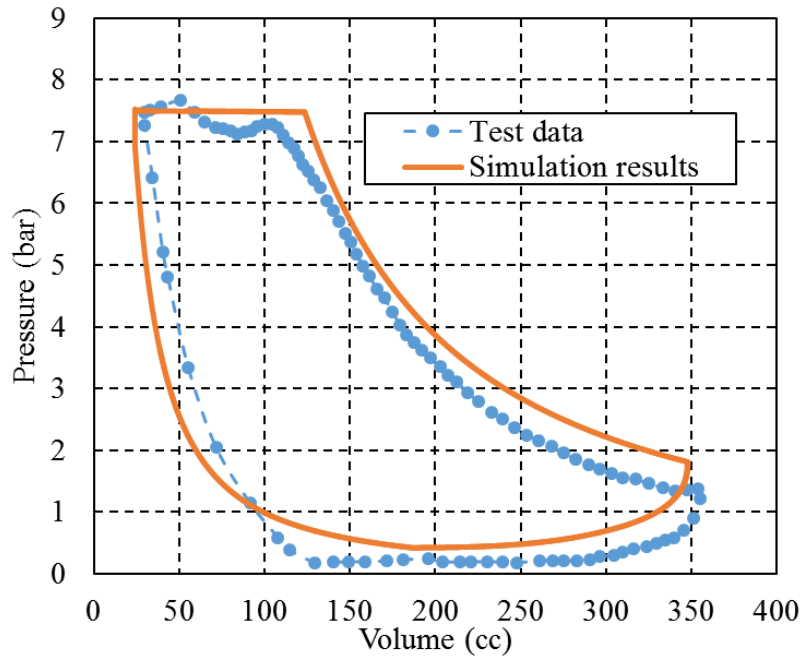
299   Figure 7. Comparison with test data from a Reciprocating Joule Engine [8]

4.3 Validation with LJEG prototype

300   **4.3 Validation with LJEG prototype**

301   The simulation model was also validated with the LJEG prototype developed at Newcastle University,

302   which is comprised of a compressor, an expander, and an external heater. Two double-acting free-

303   pistons are placed in the compressor (left) and the expander (right) respectively, which separates the

304   cylinders into two opposite chambers. The figure of the prototype is shown in Figure 8, and more

305   information can be found in elsewhere [9]. A control algorithm is developed in LabVIEW to set the

306   valve timings with the piston displacement and velocity as the feedbacks. The bore of the expander is

307   80.0 mm, with a maximum stroke of 120.0 mm. The bore of the compressor is 66.0 mm, and the bore

308   of the connection rod is 10.0 mm. The total moving mass of the system is 8.5 kg. The inlet pressure of

18

309   the expander is 2.5 bar during the testing. More details about the prototype and its configuration can

310   be found elsewhere [3, 9].
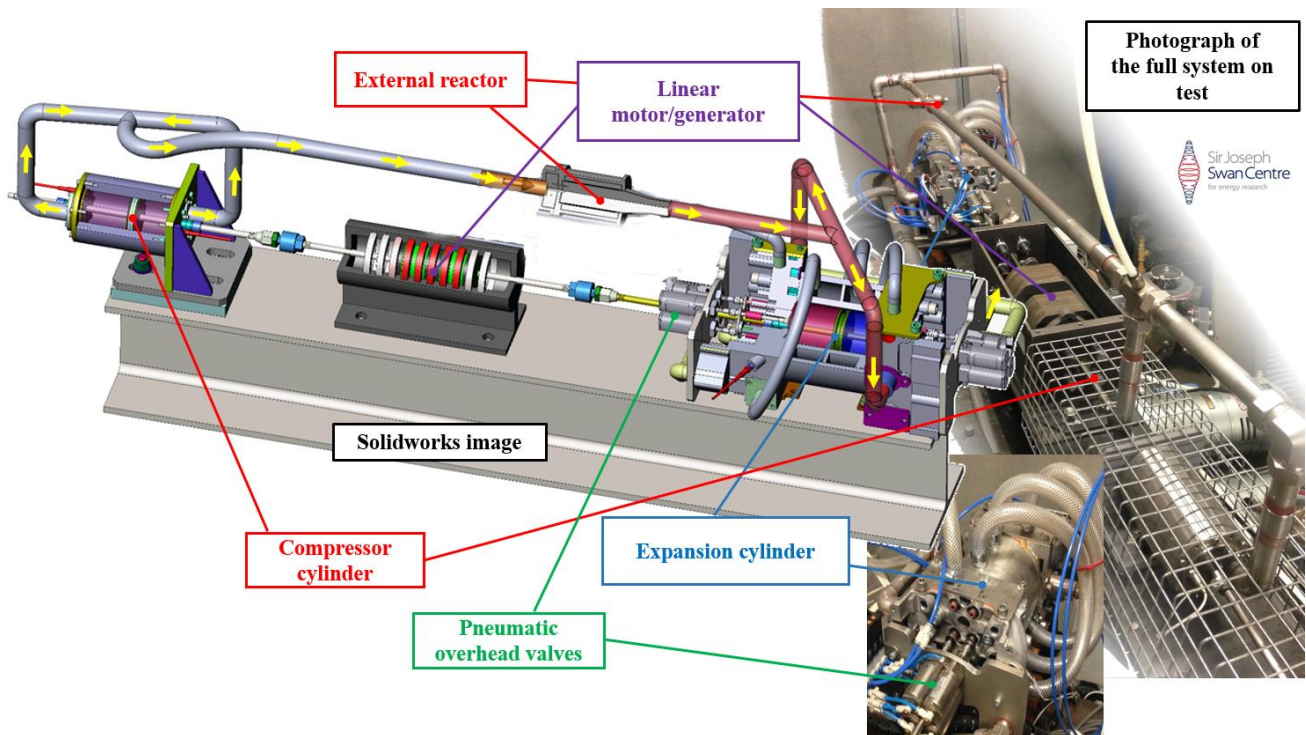
311

312   Figure 8. LJEG prototype at Newcastle University

313   The validation results on the piston displacement and the cylinder pressure in the left chamber of the

314   expander cylinder are presented in Figure 9 and Figure 10 respectively. It is found that the simulation

315   model agrees with the piston movement in the tests, and the system operating frequency fits very well.

316   The cylinder pressure profile in the expander can be precisely estimated during the compression and

317   the expansion processes. There is a difference during the intake process as a simple step function is

318   adopted to simulate the valve lifting profile, which cannot predict the gas pressure instantaneous

319   fluctuations when the valves open and close. Despite these errors, the simulation model is considered

320   to be of reasonable accuracy to estimate the operation characteristics of the LJEG system.

321
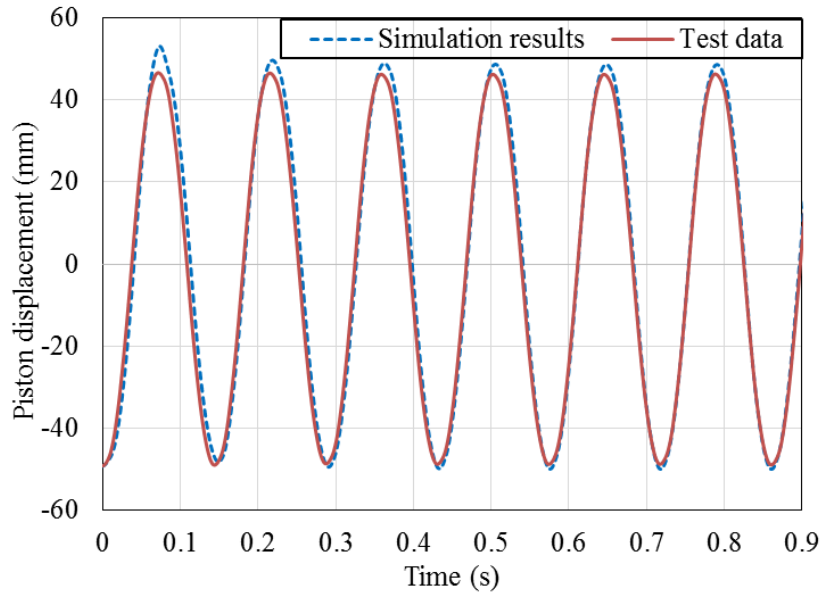
322   Figure 9. The comparison with test data from a LJEG prototype on piston displacement

323
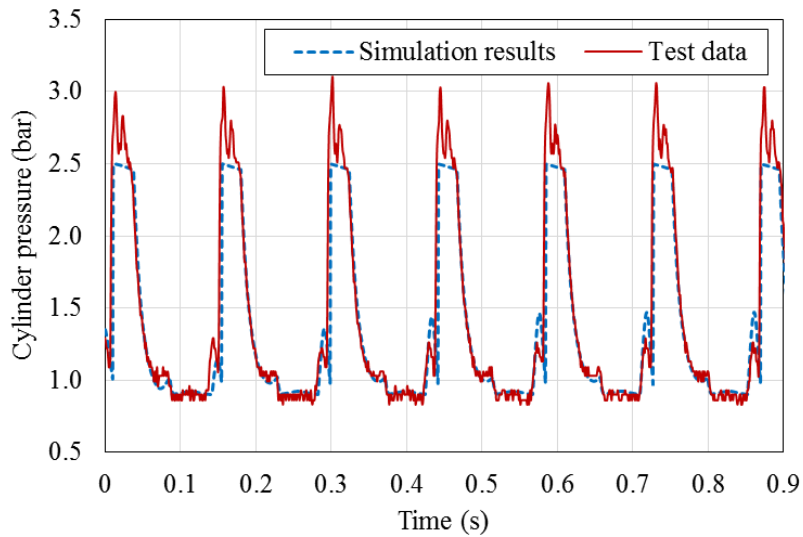
324   Figure 10. The comparison with the test data from the LJEG prototype on the cylinder pressure

5. Fundamental system performance

326   The values for the input variables during the current simulation are listed in Table 1. The inlet pressure

327   of the expander is set to 7.0 bar, which is feasible for a compressor at the end of compression process.

328   The data in Table 3 shows the system performance with the input parameter shown in Table 1. The

329   indicated power from the linear expander is estimated to be 6582.0 W, and the indicated power from

330   the linear compressor is estimated to be 1594.0 W. The electric power output can reach 4412.0 W. The

331   engine thermal efficiency can reach above 34%, with an electric generating efficiency of 30% from

332   our simulation [3, 9].

333   Table 3 LJEG system performance

Performance [Unit]	Value
Operation frequency [Hz]	15.0
Piston amplitude from central stroke [mm]	51.0
Clearance length [mm]	9.0
Peak piston velocity [m/s]	4.0
Compression ratio [-]	12.3

334   The piston displacement versus time is demonstrated in Figure 11, which shows certain similarity with

335   a sinusoidal wave with a fixed amplitude and period during stable operation process after the beginning

336   stage. The piston moves between its top dead centre (TDC) and bottom dead centre (BDC) from

337   approximately -51.0 mm to +51.0 mm. The operation stroke is around 102.0 mm, and the clearance

338   length is 9.0 mm, which can be adjusted by the valve timings, the inlet pressure of the expander, and

339   the load of the generator. As there is no combustion in the expander and the driven pressure in the

340   expander is lower (normally higher than 40 bar after combustion for an internal combustion engine),

341   the clearance length is longer than that of an internal combustion free-piston engine.

342
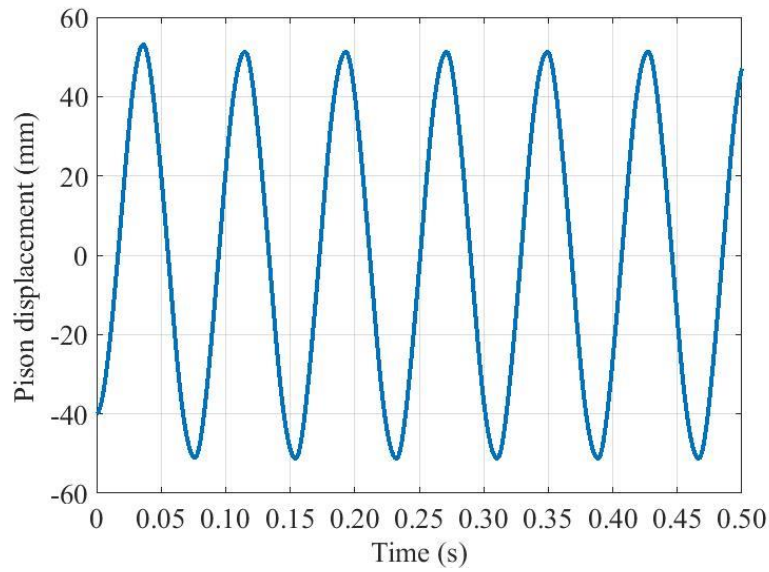
Figure 11. The piston displacement vs time

The piston velocity profile is demonstrated in Figure 12. As there is no combustion, the difference of the piston velocity during the gas intake process and the exhaust process is not significant. The piston velocity reaches its peak value before it crosses the midpoint of the stroke during the intake process. The peak piston velocity achieved is approximately 4.0 m/s, which is lower than that of a free-piston internal combustion engine with similar size (nearly 4.5 m/s) [31], due to a lower input pressure level without combustion. The corresponding system frequency is approximately 13 Hz (equivalent to 780 rpm) with the current operation conditions, which is also lower than the reported operation frequency of a free-piston internal combustion engine (20-50 Hz).

22

352
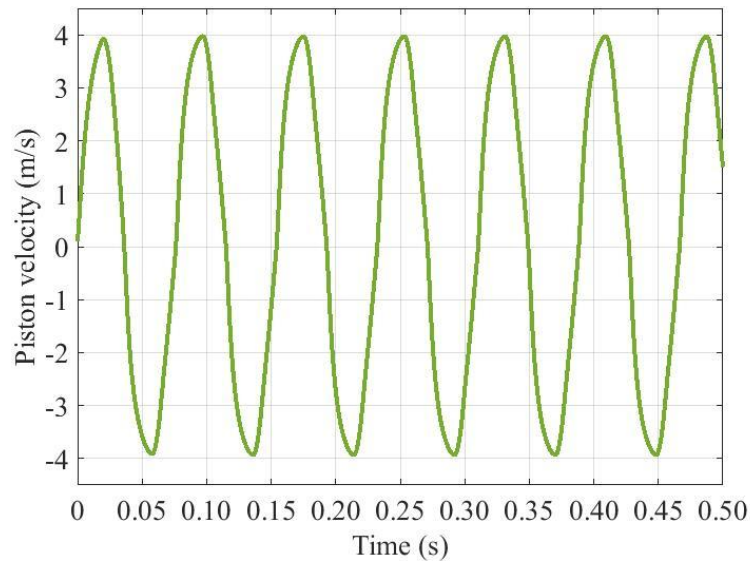
Figure 12. The piston velocity vs time

354   The pressure-displacement diagram of the left chamber of the linear expander is shown in Figure 13,

355   with the valve open/closing timing marked on it. During the simulation, the intake valve is set to open

356   when the piston reaches its TDC. The peak pressure in the expander is affected by the intake duration

357   of the expander of the other side. When the intake duration of the other side is short, then the gas

358   pressure at the end of compression process will be lower than the intake pressure, and vice versa.

359
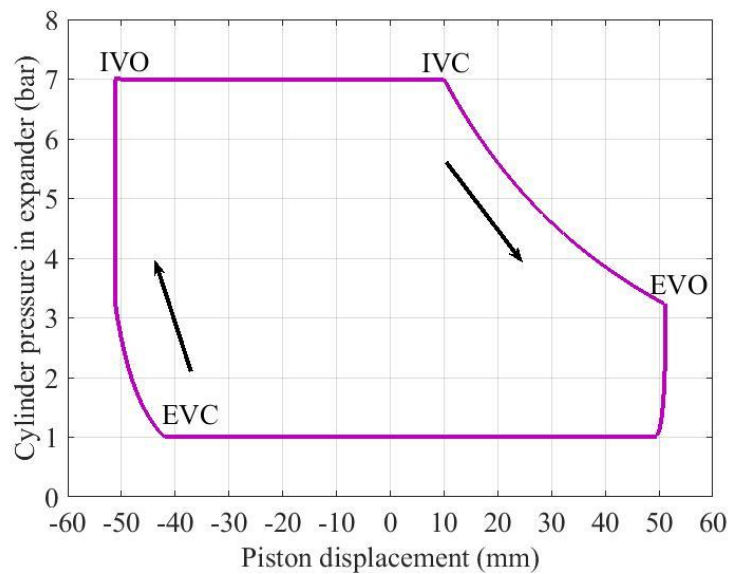
Figure 13. The pressure in the expander vs the piston displacement

361 The pressure in the left chamber of the linear compressor with piston displacement is shown in Figure

362 14, with the valve opening timing marked on it. The compression and expansion processes of the

363 compressor are assumed to be isentropic processes. Reed valves are employed in the LJEG prototype.

364 The inlet pressure for the linear compressor is equal with the ambient pressure, and the pressure in the

365 compressor is assumed to be drop to and maintain at the ambient pressure when the intake valve of the

366 compressor opens. The exhaust valve will be open when the gas pressure in the compressor reaches

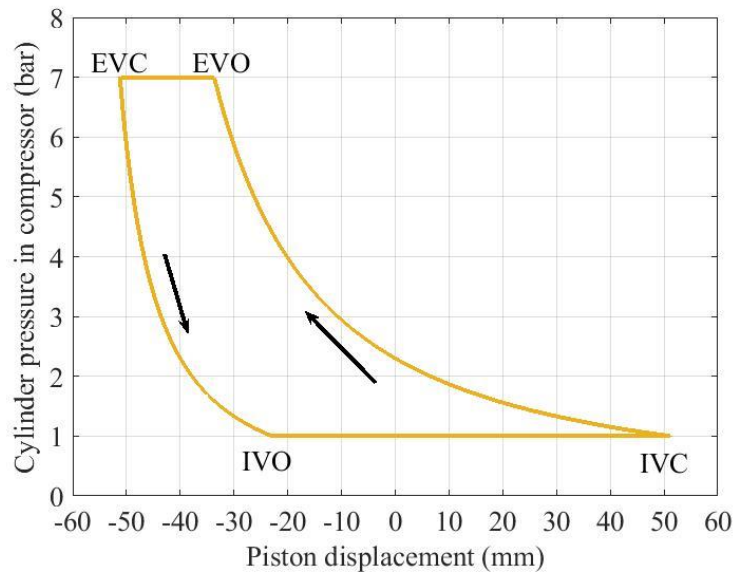367 the target pressure (7.0 bar in this simulation), and the compressor will then output the compressed gas

368 to the reactor for combustion with the fuel. The exhaust valve will be closed when the gas pressure in

369 the compressor drops below the target pressure.

371 Figure 14. Pressure in the compressor vs piston displacement

372 The forces acting on the piston that contribute to the piston inertia force are compared in Figure 15. It

373 is found that the force from the expander is highest among all the forces acting on the piston, which

374 can reach up to 3500 N. The peak force from the generator is approximately 2100 N. The peak force

375 from the compressor is 2000 N, which is achieve at the end of the compression process, and stays at

376 the peak value during the outlet process. The force from the expander will overcome the forces from

377 the compressor, the linear generator, and the frictional force, and acts as a excite force to drive the

24

378   pistons reciprocate. As the force from the expander is generated by the gas pressure in its chambers,

379   the influence of the influence pressure will be significant to the system.
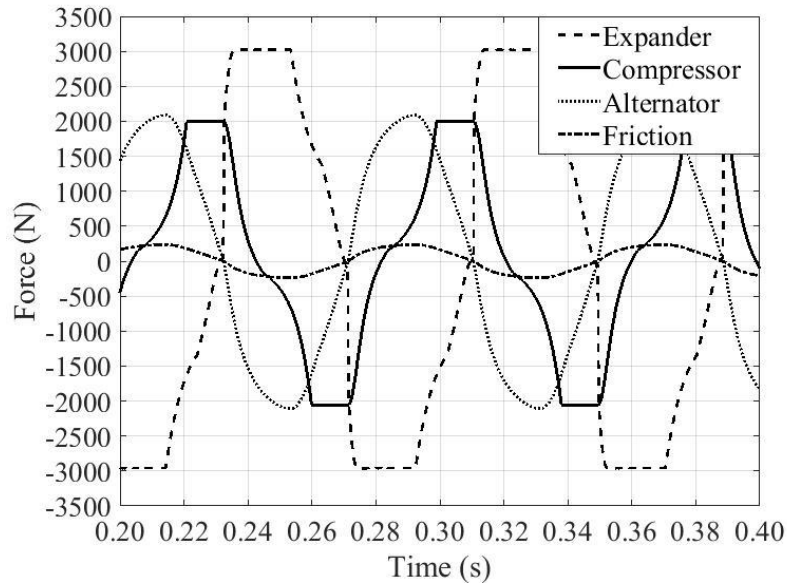
380

381   Figure 15 Forces vs time

382   The system power output with different system pressures (or the input pressure of the linear expander)

383   is shown in Figure 16, and all the other input parameters remained unchanged during the simulation.

384   Linear fittings for expander indicated power and electric power are presented in the same figure. It is

385   found that both the indicated power of the expander and the electric power of the linear alternator are

386   nearly in a linear relationship with the system pressure. When the system pressure is increased to above

387   7.5 bar, the electric power extracted from the LJEG system can be above 5.0 kW. As a result, with the

388   current setting of the system volumetric parameters and operating parameters, the indicated power of

389   the linear expander, P_{ex} (W) can be estimated by:

390                        $$P_{ex} = 1943.8 \times p_{in} - 6848.1$$ (18)

391   The electric power output of the linear alternator, P_e (W) can be estimated by:

392                        $$P_e = 1247.4 \times p_{in} - 4214.9$$ (19)

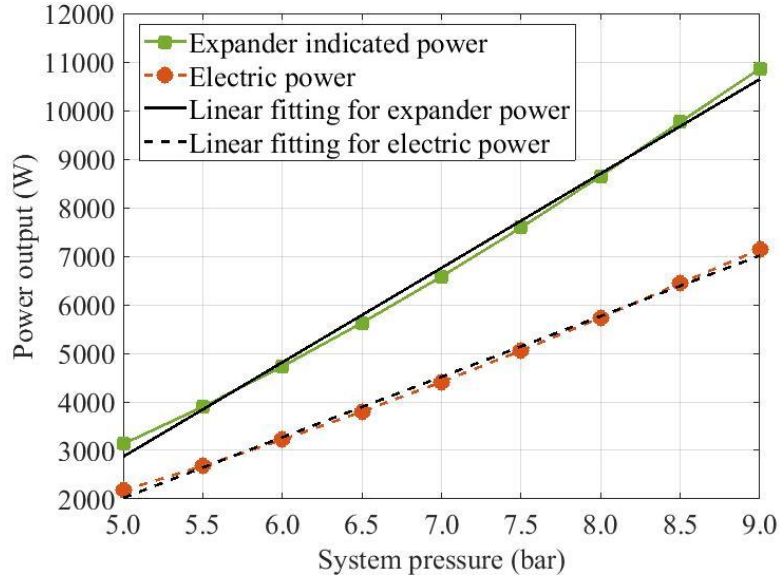393   Where p_{in} (bar) is the inlet pressure of the linear expander, or the system pressure.

25

394

395   Figure 16. Power output with different system pressures

Conclusions

397   In this research, the background and recent development of the LJEG was summarised. A detailed

398   numerical model was described, and model validation was performed with test data from both a

399   reciprocating Joule Engine and a LJEG prototype. Fundamental system operation characteristics were

400   presented. The main conclusions from this work are listed below:

401   (1) It was found that the piston displacement shows certain similarity with a sinusoidal wave with fixed

402   amplitude and period. The operation stroke is around 102.0 mm, and the clearance length is 9.0 mm.

403   (2) The peak piston velocity and system operation frequency are found to be lower than that of a free-

404   piston internal combustion engine with similar size, due to a lower input pressure level without

405   combustion. The peak piston velocity achieved is approximately 4 m/s, and the corresponding system

406   frequency is approximately 13 Hz (equivalent to 780 rpm) with the current operation conditions.

407   (3) The electric power output can reach 4.4 kW$_e$, the engine thermal efficiency can reach above 34%,

408   with an electric generating efficiency of 30%.

26

409   (4) The peak pressure in the expander is affected by the intake duration of the expander of the other

410   side. When intake duration of the other side is short, then the gas pressure at the end of compression

411   process will be lower than the intake pressure, and vice versa.

412   (5) Both the indicated power of the expander and the electric power of the linear alternator are nearly

413   in a linear relationship with the system pressure.

Acknowledgement

References

418   [1]. R. W. Moss, A. P. Roskilly, S. K. Nanda, *Reciprocating Joule-cycle engine for domestic CHP*
419   *systems.* Applied Energy, 2005. **80**(2): p. 169-185.

420   [2]. M. A. Bell, T. Partridge, *Thermodynamic design of a reciprocating Joule cycle engine.*
421   Proceedings of the Institution of Mechanical Engineers, Part A: Journal of Power and Energy,
422   2003. **217**(3): p. 239-246.

423   [3]. Rikard Mikalsen, Anthony P. Roskilly. *The free-piston reciprocating Joule Cycle engine: A*
424   *new approach to efficient domestic CHP generation*. In *Proceeding of ICAE2012 Conference.*
425   2012.

426   [4]. Rikard Mikalsen, A. P. Roskilly, *A review of free-piston engine history and applications.*
427   Applied Thermal Engineering, 2007. **27**(14): p. 2339-2352.

428   [5]. M. Razali Hanipah, R. Mikalsen, A. P. Roskilly, *Recent commercial free-piston engine*
429   *developments for automotive applications.* Applied Thermal Engineering, 2015. **75**: p. 493-
430   503.

431   [6]. Boru Jia, Andrew Smallbone, Huihua Feng, Guohong Tian, Zhengxing Zuo, A. P. Roskilly, *A*
432   *fast response free-piston engine generator numerical model for control applications.* Applied
433   Energy, 2016. **162**: p. 321-329.

434   [7]. Boru Jia, Guohong Tian, Huihua Feng, Zhengxing Zuo, A. P. Roskilly, *An experimental*
435   *investigation into the starting process of free-piston engine generator.* Applied Energy, 2015.
436   **157**: p. 798-804.

437   [8]. Robert William Allen. *The reciprocating joule cycle engine for micro combined heat and*
438   *power applications*. University of Plymouth. 2008.

439   [9]. Dawei Wu, Anthony P. Roskilly, *Design and parametric analysis of linear Joule-cycle engine*
440   *with out-of-cylinder combustion.* Energy Procedia, 2014. **61**: p. 1111-1114.

441 [10]. Muriel Alaphilippe, Sébastien Bonnet, Pascal Stouffs, *Low power thermodynamic solar energy*
442 *conversion: coupling of a parabolic trough concentrator and an Ericsson engine.* International
443 Journal of Thermodynamics, 2007. **10**(1): p. 37-45.

444 [11]. Jerzy Wojewoda, Zbyszko Kazimierski, *Numerical model and investigations of the externally*
445 *heated valve Joule engine.* Energy, 2010. **35**(5): p. 2099-2108.

446 [12]. M. Creyx, E. Delacourt, C. Morin, B. Desmet, P. Peultier, *Energetic optimization of the*
447 *performances of a hot air engine for micro-CHP systems working with a Joule or an Ericsson*
448 *cycle.* Energy, 2013. **49**: p. 229-239.

449 [13]. Robert William Allen, *The reciprocating joule cycle engine for micro combined heat and*
450 *power applications.* 2008.

451 [14]. Chendong Guo, Huihua Feng, Boru Jia, Zhengxing Zuo, Yuyao Guo, Tony Roskilly, *Research*
452 *on the operation characteristics of a free-piston linear generator: Numerical model and*
453 *experimental results.* Energy Conversion and Management, 2017. **131**: p. 32-43.

454 [15]. Yaodong Wang, Lin Chen, Boru Jia, Anthony Paul Roskilly, *Experimental study of the*
455 *operation characteristics of an air-driven free-piston linear expander.* Applied Energy, 2017.
456 **195**: p. 93-99.

457 [16]. Boru Jia, Andrew Smallbone, Zhengxing Zuo, Huihua Feng, Anthony Paul Roskilly, *Design*
458 *and simulation of a two-or four-stroke free-piston engine generator for range extender*
459 *applications.* Energy Conversion and Management, 2016. **111**: p. 289-298.

460 [17]. Boru Jia, Zhengxing Zuo, Huihua Feng, Guohong Tian, A. P. Roskilly, *Development approach*
461 *of a spark-ignited free-piston engine generator.* 2014, SAE Technical Paper.

462 [18]. Boru Jia, Zhengxing Zuo, Huihua Feng, Guohong Tian, A. P. Roskilly, *Investigation of the*
463 *starting process of free-piston engine generator by mechanical resonance.* Energy Procedia,
464 2014. **61**: p. 572-577.

465 [19]. Chia-Jui Chiang, Jing-Long Yang, Shao-Ya Lan, Tsung-Wei Shei, Wen-Shu Chiang, Bo-Liang
466 Chen, *Dynamic modeling of a SI/HCCI free-piston engine generator with electric mechanical*
467 *valves.* Applied energy, 2013. **102**: p. 336-346.

468 [20]. Terry A. Johnson, Michael T. Leick, Ronald W. Moses, *Experimental evaluation of the free*
469 *piston engine-linear alternator (FPLA).* Sandia National Laboratories, 2015.

470 [21]. Stephan Schneider, Horst E. Friedrich, *Experimental Investigation and Analysis of*
471 *Homogeneous Charge Compression Ignition in a Two-Stroke Free-Piston Engine.* SAE
472 International Journal of Engines, 2015. **9**(2015-32-0706): p. 365-373.

473 [22]. Zhenfeng Zhao, Fujun Zhang, Ying Huang, Changlu Zhao, *Determination of TDC in a*
474 *hydraulic free-piston engine by a novel approach.* Applied Thermal Engineering, 2014. **70**(1):
475 p. 524-530.

476 [23]. Shigeaki Goto, Kaznunari Moriya, Hidemasa Kosaka, Tomoyuki Akita, Yoshihiro Hotta,
477 Takaji Umeno, Kiyomi Nakakita, *Development of free piston engine linear generator system*
478 *part 2-investigation of control system for generator.* 2014, SAE Technical Paper.

479 [24]. Hidemasa Kosaka, Tomoyuki Akita, Kazunari Moriya, Shigeaki Goto, Yoshihiro Hotta, Takaji
480 Umeno, Kiyomi Nakakita, *Development of free piston engine linear generator system Part 1-*
481 *investigation of fundamental characteristics.* 2014, SAE Technical Paper.

482 [25]. Roman Virsik, Alex Heron. *Free piston linear generator in comparison to other range-
483 extender technologies*. In *Electric Vehicle Symposium and Exhibition (EVS27), 2013 World*.
484 2013. IEEE.

485 [26]. Stephan Schneider, Frank Rinderknecht, Horst E. Friedrich. *Design of future concepts and
486 variants of The Free Piston Linear Generator*. In *Ecological Vehicles and Renewable Energies
487 (EVER), 2014 Ninth International Conference on*. 2014. IEEE.

488 [27]. Florian Kock, Frank Rinderknecht, *A high efficient energy converter for a hybrid vehicle
489 concept-gas spring focused*. Tagungsband EVER 12, 2012.

490 [28]. Cornelius Ferrari, Horst E. Friedrich. *Development of a Free-Piston Linear Generator for use
491 in an Extended-Range Electric Vehicle*. In *Proc. Symposium EVS26, Los Angeles, USA*. 2012.

492 [29]. Yan-xiao Li, Zheng-xing Zuo, Hui-hua Feng, Bo-ru Jia, *Parameters matching requirements
493 for diesel free piston linear alternator start-up*. Advances in Mechanical Engineering, 2015.
494 **7**(3): p. 1687814015574408.

495 [30]. Yuxi Miao, Zhengxing Zuo, Huihua Feng, Chendong Guo, Yu Song, Boru Jia, Yuyao Guo,
496 *Research on the combustion characteristics of a free-piston gasoline engine linear generator
497 during the stable generating process*. Energies, 2016. **9**(8): p. 655.

498 [31]. Boru Jia, Zhengxing Zuo, Guohong Tian, Huihua Feng, A. P. Roskilly, *Development and
499 validation of a free-piston engine generator numerical model*. Energy Conversion and
500 Management, 2015. **91**: p. 333-341.

501 [32]. Boru Jia, Zhengxing Zuo, Huihua Feng, Guohong Tian, Andrew Smallbone, A. P. Roskilly,
502 *Effect of closed-loop controlled resonance based mechanism to start free piston engine
503 generator: Simulation and test results*. Applied Energy, 2016. **164**: p. 532-539.

504 [33]. Huihua Feng, Chendong Guo, Boru Jia, Zhengxing Zuo, Yuyao Guo, Tony Roskilly, *Research
505 on the intermediate process of a free-piston linear generator from cold start-up to stable
506 operation: Numerical model and experimental results*. Energy Conversion and Management,
507 2016. **122**: p. 153-164.

508 [34]. Mohd Razali Hanipah. *Development of a spark ignition free-piston engine generator*.
509 Newcastle University. 2015.

510 [35]. Boru Jia. *Analysis and control of a spark ignition free-piston engine generator*. Newcastle
511 University. 2016.

512 [36]. Boru Jia, Andrew Smallbone, Rikard Mikalsen, Huihua Feng, Zhengxing Zuo, Anthony Paul
513 Roskilly, *Disturbance analysis of a free-piston engine generator using a validated fast-
514 response numerical model*. Applied Energy, 2017. **185**: p. 440-451.

515 [37]. Boru Jia, Rikard Mikalsen, Andrew Smallbone, Zhengxing Zuo, Huihua Feng, Anthony Paul
516 Roskilly, *Piston motion control of a free-piston engine generator: A new approach using
517 cascade control*. Applied Energy, 2016. **179**: p. 1166-1175.

518 [38]. Dawei Wu, Aslan Sa Jalal, Nick Baker, *A Coupled Model of the Linear Joule Engine with
519 Embedded Tubular Permanent Magnet Linear Alternator*. Energy Procedia, 2017. **105**: p.
520 1986-1991.

521 [39]. Yunus A. Cengel, Michael A. Boles, *Thermodynamics: an engineering approach*. Sea, 2002.
522 **1000**: p. 8862.

523 [40]. Günter F. Hohenberg, *Advanced approaches for heat transfer calculations*. 1979, SAE
524 Technical paper.

525   [41].   John B. Heywood, *Internal combustion engine fundamentals*. Vol. 930. 1988: Mcgraw-hill
526   New York.

527   [42].   Chang-ping Lee. *Turbine-compound free-piston linear alternator engine*. University of
528   Michigan. PhD Dissertation, 2014.

529